



1

## 2 **Determination of vadose and saturated-zone nitrate lag times using long-** 3 **term groundwater monitoring data and statistical machine learning**

4 Martin J. Wells<sup>1,3</sup>, Troy E. Gilmore<sup>2,3</sup>, Natalie Nelson<sup>4,5</sup>, Aaron Mittelstet<sup>3</sup>, John Karl Böhlke<sup>6</sup>,

5 <sup>1</sup>currently at Natural Resources Conservation Service, Redmond, OR, 97756, USA

6 <sup>2</sup>Conservation and Survey Division - School of Natural Resources, University of Nebraska, Lincoln, NE, 68583, USA

7 <sup>3</sup>Biological Systems Engineering, University of Nebraska, Lincoln, NE, 68583, USA

8 <sup>4</sup>Biological and Agricultural Engineering, North Carolina State University, Raleigh, NC, 27695, USA

9 <sup>5</sup>Center for Geospatial Analytics, North Carolina State University, Raleigh, NC, 27695, USA

10 <sup>6</sup>U.S. Geological Survey, Reston, VA, 20192, USA

11 *Correspondence to:* Troy E. Gilmore (gilmore@unl.edu)

12 **Abstract.** In this study, we explored the use of statistical machine learning and long-term groundwater nitrate monitoring data to  
13 estimate vadose-zone and saturated-zone lag times in an irrigated alluvial agricultural setting. Unlike most previous statistical  
14 machine learning studies that sought to predict groundwater nitrate concentrations within aquifers, the focus of this study was to  
15 leverage available groundwater nitrate concentrations and other environmental variable data to determine mean vertical velocities  
16 (transport rates) of water and solutes in the vadose zone and saturated zone (3.50 m/year and 3.75 m/year, respectively). Although  
17 a saturated-zone velocity that is greater than a vadose-zone velocity would be counterintuitive in most aquifer settings, the statistical  
18 machine learning results are consistent with two contrasting primary recharge processes in this aquifer: (1) diffuse recharge from  
19 irrigation and precipitation across the landscape, and (2) focused recharge from leaking irrigation conveyance canals. The vadose-  
20 zone mean velocity yielded a mean recharge rate (0.46 m/year) consistent with previous estimates from groundwater age-dating in  
21 shallow wells (0.38 m/year). The saturated zone mean velocity yielded a recharge rate (1.31 m/year) that was more consistent with  
22 focused recharge from leaky irrigation canals, as indicated by previous results of groundwater age-dating in intermediate-depth  
23 wells (1.22 m/year). Collectively, the statistical machine-learning model results are consistent with previous observations of  
24 relatively high-water fluxes and short transit times for water and nitrate in the aquifer. Partial dependence plots from the model  
25 indicate a sharp threshold where high groundwater nitrate concentrations are mostly associated with total travel times of seven  
26 years or less, possibly reflecting some combination of recent management practices and a tendency for nitrate concentrations to be  
27 higher in diffuse infiltration recharge than in canal leakage water. Limitations to the machine learning approach include potential  
28 non-uniqueness when comparing model performance for different transport rate combinations and highlight the need to corroborate  
29 statistical model results with a robust conceptual model and complementary information such as groundwater age.

30

31

32

33

34

35



## 36 1 Introduction

37 Lag times for movement of non-point source nitrate contamination through the subsurface are widely recognized (Böhlke,  
38 2002; Meals et al., 2010; Puckett et al., 2011; Van Meter and Basu, 2017) but difficult to measure. Vadose and saturated-zone lag  
39 times are of critical importance for monitoring, regulating, and managing the transport of contaminants in groundwater. However,  
40 transport time-scales are often generalized spatially and/or temporally for groundwater systems impacted by agricultural activities  
41 (Gilmore et al., 2016; Green et al., 2018; Puckett et al., 2011), resulting in a simplified groundwater management approach.  
42 Regulators and stakeholders in agricultural landscapes are increasingly in need of more precise and local lag time information to  
43 better evaluate and apply regulations and best management practices for the reduction of groundwater nitrate concentrations (e.g.,  
44 Eberts et al., 2013).

45 Field-based studies of lag times commonly use expensive groundwater age-dating techniques and/or vadose-zone  
46 sampling to estimate nitrate transport rates moving into and through aquifers (Böhlke et al., 2002, 2007; Böhlke and Denver, 1995;  
47 Browne and Guldán, 2005; Kennedy et al., 2009; McMahon et al., 2006; Morgenstern et al., 2015; Turkeltaub et al., 2016; Wells  
48 et al., 2018). Detailed process-based modelling studies focused on lag times require complex numerical models combined with  
49 spatially intensive and/or costly hydrogeological observations (Ilampooranan et al., 2019; Rossman et al., 2014; Russoniello et al.,  
50 2016). Thus, efficient but locally-applicable modelling approaches are needed (Green et al., 2018; Liao et al., 2012; Van Meter  
51 and Basu, 2015). In this study, an alternative data-driven approach (Random Forest Regression) leverages existing long-term  
52 groundwater nitrate concentration (referred to as  $[\text{NO}_3^-]$  hereafter) data and easily accessible environmental data to estimate vadose  
53 and saturated-zone vertical velocities (transport rates) for the determination of subsurface lag times.

54 Statistical machine learning methods, including Random Forest, have been used successfully for modelling  $[\text{NO}_3^-]$   
55 distribution in aquifers (Anning et al., 2012; Nolan et al., 2014; Ouedraogo et al., 2017; Rodriguez-Galiano et al., 2014; Wheeler  
56 et al., 2015), but there has not been robust analysis of model capabilities for estimating vadose and/or saturated-zone lag times.  
57 Proxies for lag time, such as well screen depth, have been used as predictors in Random Forest models (Nolan et al., 2014; Wheeler  
58 et al., 2015). Decadal lag times have been suggested from using time-averaged nitrogen inputs as predictors (e.g., 1978-1990 inputs  
59 vs 1992-2006 inputs) and by comparing their relative importance in the model (Wheeler et al., 2015). Application of similar  
60 machine learning methods suggested groundwater age could be used as a predictor to improve model performance (Ransom et al.,  
61 2017). Hybrid models, using both mechanistic models and machine learning, have also sought to integrate vertical transport model  
62 parameters and outputs to evaluate nitrate-related predictors, including vadose-zone travel times (Nolan et al., 2018).

63 The objective of this study is to test a data-driven approach for estimating vadose (unsaturated zone) and groundwater  
64 (saturated zone) transport rates and lag times for an intensively monitored alluvial aquifer in western Nebraska (Böhlke et al.,  
65 2007; Verstraeten et al., 2001b, 2001a; Wells et al., 2018). Results are compared to the hydrogeologic, mechanistic understanding  
66 from previous groundwater studies to determine strengths and weaknesses of the approach as (1) a stand-alone technique, or (2) as  
67 an exploratory analysis to guide or complement more complex physical-based models or intensive hydrogeologic field  
68 investigations.

## 69 2 Methods

### 70 2.1 Site Descriptions

71 The Dutch Flats study area is located in the western Nebraska counties of Scotts Bluff and Sioux (Fig. 1). The North  
72 Platte River delivers large quantities of water for crop irrigation in this region and runs along the southern portion of this study  
73 area. Several previous Dutch Flats area studies have investigated groundwater characteristics and provided thorough site



74 descriptions of the semi-arid region (Babcock et al., 1951; Böhlke et al., 2007; Verstraeten et al., 2001a, 2001b; Wells et al., 2018).  
75 The Dutch Flats area overlies an alluvial aquifer characterized by unconsolidated deposits of predominantly sand and gravel, with  
76 the aquifer base largely consisting of consolidated deposits of the Brule Formation (Verstraeten et al., 1995). Irrigation water not  
77 derived from the North Platte River is typically pumped from the alluvial aquifer, or water-bearing units of the Brule Formation.

78 The total area of the Dutch Flats study area is roughly 540 km<sup>2</sup>, of which approximately 290 km<sup>2</sup> (53.5%) is agricultural  
79 land (cultivated crops and pasture). Most agricultural land is concentrated south of the Interstate Canal (Homer et al., 2015). Due  
80 to the combination of intense agriculture and low annual precipitation, producers in Dutch Flats rely on a network of irrigation  
81 canals to supply water to the region. From 1908 to 2016, mean precipitation of 390 mm was measured at the nearby Western  
82 Regional Airport in Scottsbluff, NE (NOAA, 2017).

83 While some groundwater is withdrawn for irrigation, and some irrigated acres in the study area are classified as  
84 commingled (groundwater and surface water source), Scotts Bluff County irrigation is mostly from surface water sources.  
85 Estimates determined every five years suggest surface water provided between 76.8% to 98.6% of the total water withdrawals from  
86 1985 to 2015, or about 92% on average (Dieter et al., 2018). Canals transport water from the North Platte River to fields throughout  
87 the study area. Large canals in Dutch Flats include the Mitchell-Gering, Tri-State, and Interstate Canals, with the latter holding the  
88 largest water right of 44.5 m<sup>3</sup>/s. (NEDNR, 2009). Leakage from these canals provides a source of artificial groundwater recharge.  
89 Previous studies estimate the leakage potential of canals in the region results in as much as 40% to 50% of canal water being lost  
90 during conveyance (Ball et al., 2006; Harvey and Sibray, 2001; Hobza and Andersen, 2010; Luckey and Cannia, 2006). Leakage  
91 estimates from a downstream section of the Interstate Canal (extending to the east of the study area; Hobza and Andersen (2010))  
92 suggest fluxes ranging from 0.08 to 0.7 m day<sup>-1</sup> through the canal bed. Assuming leakage of 0.39 m day<sup>-1</sup> leakage over the Interstate  
93 Canal bed area (16.8 m width x 55.5 km length) within Dutch Flats yields 4.1 x 10<sup>5</sup> m<sup>3</sup> day<sup>-1</sup> of leakage. Applied over an on-  
94 average 151-day operation period (USBR, 2018), leakage from Interstate Canal alone could approach 6.1 x 10<sup>7</sup> m<sup>3</sup> annually, or  
95 about 29% of the annual volume of precipitation in the Dutch Flats area.

96 A 1990s study investigated both spatial and temporal influences from canals in the Dutch Flats area (Verstraeten et al.,  
97 2001b, 2001a), with results later synthesized by Böhlke et al. (2007). Canals were found to dilute groundwater [NO<sub>3</sub><sup>-</sup>] near canals  
98 with low-[NO<sub>3</sub><sup>-</sup>] (e.g., [NO<sub>3</sub><sup>-</sup>] < 0.06 mg N L<sup>-1</sup> in 1997) canal water during irrigation season. <sup>3</sup>H/<sup>3</sup>He age-dating was used to  
99 determine apparent groundwater ages and recharge rates. It was noted that wells near canals displayed evidence of high recharge  
100 rates influenced by local canal leakage. Data from wells far from the canals indicated that shallow groundwater was more likely  
101 influenced by local irrigation practices (i.e., furrows in fields), while deeper groundwater was impacted by both localized irrigation  
102 and canal leakage (Böhlke et al., 2007). Shallow groundwater in the Dutch Flats area has stable isotope composition consistent  
103 with surface water sources (i.e., North Platte River; (Böhlke et al., 2007; Cherry et al., 2020)).

104 The Dutch Flats area is within the North Platte Natural Resources District (NPNRD), which is 1 of 23 groundwater  
105 management districts in Nebraska tasked with, among other functions, promoting efforts to improve water quality and quantity.  
106 The NPNRD has a large monitoring well network consisting of 797 wells, 327 of which are nested. Nested well clusters are drilled  
107 and constructed such that screen intervals represent shallow groundwater intersecting the water table (screen length = 6.1 m),  
108 intermediate aquifer depths (screen length = 1.5 m), and deep groundwater near the base of the unconfined aquifer (screen length  
109 = 1.5 m).

110 Influenced by both regulatory and economic incentives, the Dutch Flats area has undergone a notable shift in irrigation  
111 practices in the last two decades. From 1999 to 2017, center pivot irrigated area has increased by approximately 270%, from  
112 roughly 3,830 hectares to 14,253 hectares, or from 13% to 49% of the total agricultural land area, respectively. The majority of  
113 this shift in technology has occurred on fields previously irrigated by furrow irrigation. Conventional furrow irrigation has an



114 estimated potential application efficiency (“measure of the fraction of the total volume of water delivered to the farm or field to  
115 that which is stored in the root zone to meet the crop evapotranspiration needs,” per Irmak et al. (2011)) of 45% to 65%, compared  
116 to center pivot sprinklers at 75% to 85% (Irmak et al., 2011). Based on improved irrigation efficiency (between 10–40%), average  
117 precipitation throughout growing season (29.5 cm for 15 April to 13 October (Yonts, 2002)), and average water requirements for  
118 corn (69.2 cm (Yonts, 2002)), converting furrow irrigated fields to center pivot over the aforementioned 14,253 hectares could  
119 represent a difference of  $1 \times 10^7 \text{ m}^3$  to  $6 \times 10^7 \text{ m}^3$  in water applied. Those (roughly approximated) differences in water volumes are  
120 equivalent to 6–28% of average annual precipitation applied over the Dutch Flats area, suggesting the change in irrigation practice  
121 does have potential to alter the water balance in the area.

122 The hypothesis of lower recharge due to changes in irrigation technology was investigated by Wells et al. (2018) by  
123 comparing samples collected in 1998 and 2016. While mean recharge rate was not significantly different, a lower recharge rate  
124 was indicated by data from 88% of the wells. Long-term Dutch Flats  $[\text{NO}_3^-]$  trends were also assessed in the study, suggesting  
125 decreasing trends (though statistically insignificant) from 1998 to 2016 throughout the Dutch Flats area, and nitrogen isotopes of  
126 nitrate indicated little change in biogeochemical processes. For additional background, Wells et al., (2018) provides a more in-  
127 depth analysis of recent  $[\text{NO}_3^-]$  trends in this region (see also, Fig. S1, which shows only the nitrate data used in the present study).

128 Other long-term changes to the landscape have included statistically significant reductions in mean fertilizer application  
129 rates (1987–1999 vs. 2000–2012) and volume of water diverted into the Interstate Canal (1983–1999 vs. 2000–2016), while a  
130 significant increase in area of planted corn was found (1983–1999 vs. 2000–2016). Precipitation was also evaluated, and though  
131 the mean has decreased over a similar time period, it was not statistically significant.

## 132 2.2 Statistical Machine Learning Modelling Framework

133 Statistical machine learning uses algorithms to assess and identify complex relationships between variables. Learned  
134 relations can be used to uncover nonlinear trends in data that might otherwise be overshadowed when using simple regression  
135 techniques (Hastie et al., 2009). In this study we used Random Forest Regression, where Random Forests are created by combining  
136 hundreds of unskilled regression trees into one model ensemble, or “forest”, which collectively produce skilled and robust  
137 predictions (Breiman, 2001). Predictors used in the model represent site-specific explanatory variables (e.g., precipitation, vadose-  
138 zone thickness, depth to bottom of screen, etc.) that may impact the response variable, groundwater  $[\text{NO}_3^-]$ .

## 139 2.3 Random Forest Application

140 Random Forest regression models of groundwater  $[\text{NO}_3^-]$  were developed using five-fold cross validation (Hastie et al.,  
141 2009), where four folds were used to build the model (training data), and one fold was held out (testing data). The maximum and  
142 minimum of the  $[\text{NO}_3^-]$  and each predictor were determined and placed into each fold for training models to eliminate the potential  
143 for extrapolation during validation. Each fold was used as training data four times, and testing data once. This process was repeated  
144 five times to create a total of 25 models, similar to the approach used by Nelson et al. (2018). The four folds designated to build  
145 the model underwent a nested five-fold cross validation, as specified in the *trainControl* function within the *caret* (Classification  
146 and Regression Training) R package (Kuhn, 2008; R Core Team, 2017). Functions in *caret* were used to train the Random Forest  
147 models.

148 To evaluate model performance, Nash-Sutcliffe Efficiency (NSE), permutation importance, and partial dependence were  
149 quantified. NSE indicates the degree to which observed and predicted values deviate from a 1:1 line, and ranges from negative  
150 infinity to 1 (Nash and Sutcliffe, 1970).



$$151 \quad NSE = 1 - \frac{\sum_{i=1}^n (Y_i^{obs} - Y_i^{pred})^2}{\sum_{i=1}^n (Y_i^{obs} - Y^{mean})^2}, \quad (1)$$

152 where  $n$  is the number of observations,  $Y_i^{obs}$  is the  $i^{\text{th}}$  observation of the response variable ( $[\text{NO}_3^-]$ ),  $Y_i^{pred}$  is the  $i^{\text{th}}$  prediction from  
153 the Random Forest model, and  $Y^{mean}$  is the mean of observations  $i$  through  $n$ . Values from negative infinity to 0 suggest the mean  
154 of the observed  $[\text{NO}_3^-]$  would serve as a better predictor than the model. When  $NSE = 0$ , model predictions are as accurate as that  
155 of a model with only the mean observed  $[\text{NO}_3^-]$  as a predictor. From 0, larger NSE values indicate a model's predictive ability  
156 improves, until  $NSE = 1$ , where observations and predictions are equal. NSE was calculated for both the training and testing data.

157 For each tree, a random bootstrapped sample is extracted from the dataset (Efron, 1979), as well as a random subset of  
158 predictors to consider fitting at each split. Thus, each tree is grown from a bootstrap sample and random subset of predictors,  
159 making trees random and grown independent of the others. Observations not used as bootstrap samples are termed out-of-bag data  
160 (OOB).

161 When building a tree, all  $[\text{NO}_3^-]$  from the bootstrap sample are categorized into terminal nodes, such that each node is  
162 averaged and yields a predicted  $[\text{NO}_3^-]$ . The performance and mean squared error (MSE) of a Random Forest model is evaluated  
163 by comparing the observed  $[\text{NO}_3^-]$  of the OOB data to the average predicted  $[\text{NO}_3^-]$  from the forest. OOB data from the training  
164 dataset may be used to evaluate both permutation importance, referred to in the rest of this text as variable importance, and partial  
165 dependence. Variable importance uses percent increase in mean squared error ( $\%_{\text{incMSE}}$ ) to describe predictive power of each  
166 predictor in the model (Jones and Linder, 2015). During this process, a single predictor is permuted, or shuffled, in the dataset.  
167 Therefore, each observed  $[\text{NO}_3^-]$  has the same relationship between itself and all predictors, except one permuted variable. The  
168  $\%_{\text{incMSE}}$  of a variable is determined by comparing the permuted OOB MSE to unpermuted OOB MSE. Important predictors will  
169 result in a large  $\%_{\text{incMSE}}$ , while a variable of minor importance does little to impact a model's performance, as suggested by a low  
170  $\%_{\text{incMSE}}$  value.

171 Partial dependence curves serve as a graphical representation of the relationship between  $[\text{NO}_3^-]$  and predictors in the  
172 Random Forest model ensemble (Hastie et al., 2009). Each plot considers the effects of other variables in the model, since  
173 predictions of  $[\text{NO}_3^-]$  are influenced by several predictors when building each tree. In these models, the y-axis of a partial  
174 dependence plot represents the average of the OOB predicted  $[\text{NO}_3^-]$  at a specific x-value of each predictor.

## 175 2.4 Variables and Project Setup

176 Data from 15 predictors were collected and analysed (Table 1). Spatial variables were manipulated using ArcGIS 10.4.  
177 The  $[\text{NO}_3^-]$  dataset for the entire NPNRD had 10,676 observations from 1979 to 2014, and was downloaded from the Quality-  
178 Assessed Agrichemical Contaminant Database for Nebraska Groundwater (University of Nebraska-Lincoln, 2016). Spatial  
179 locations for each well were included in the original  $[\text{NO}_3^-]$  dataset and imported into GIS. Wells were clipped to the Dutch Flats  
180 model area, resulting in 2,829  $[\text{NO}_3^-]$  observations from 214 wells. In order to have an accurate vadose-zone thickness, only wells  
181 with a corresponding depth to groundwater record, of which the most recent record was used, were selected (2,651 observations  
182 from 172 wells). Over this period, several wells were sampled much more frequently than others (e.g., monthly sampling, over a  
183 short period of record), especially during a USGS National Water-Quality Assessment (NAWQA) study from 1995 to 1999. In  
184 order to prevent those wells from dominating the training and testing of the model, annual median  $[\text{NO}_3^-]$  was calculated for each  
185 well and used in the dataset. The dataset was further manipulated such that each median  $[\text{NO}_3^-]$  observation had 15 complementary  
186 predictors (Table 1). The selected predictor variables capture drivers of long-term  $[\text{NO}_3^-]$  and  $[\text{NO}_3^-]$  lags. After incorporating all  
187 data, including limited records of dissolved oxygen (DO), the final dataset included 1,049  $[\text{NO}_3^-]$  observations from 162 wells



188 sampled between 1993 and 2013. Additional details of the data selection, sources, and manipulations may be found in the  
189 supplemental material.

190 Predictors were divided into two categories; static and dynamic (Table 1). Static predictors are those that either do not  
191 change over the period of record, or annual records were limited. DO, for example, could potentially experience slight annual  
192 variations, but data were not available to assign each nitrate sample a unique DO value. Instead, observations for each well were  
193 assigned the average DO value observed from the well. This approximation was considered reasonable because nitrate isotopic  
194 composition and DO data collected in the 1990s and by Wells et al. (2018) did not indicate any major changes to biogeochemical  
195 processes over nearly two decades. Total travel time was strictly considered a static predictor in this study and was used to link the  
196 nitrate-sampling year to a dynamic predictor value.

197 Dynamic predictors were defined in this study as data that changed temporally over the study period. Therefore, each  
198 annual median  $[\text{NO}_3^-]$  was assigned a lagged dynamic value to represent the difference between the time of a particular surface  
199 activity (e.g., timing of a particular irrigation practice) and when groundwater sampling occurred. Dynamic predictors were  
200 available from 1946 to 2013 and included annual precipitation, Interstate Canal discharge, area under center pivot sprinklers, and  
201 area of planted corn (Fig. 2). Dynamic predictors were included to assess their ability to optimize Random Forest groundwater  
202 modelling and determine an appropriate lag time. Lag times were based on the vertical travel distance through both the vadose and  
203 saturated zones. Area of planted corn was included as a proxy for fertilizer data, which were unavailable prior to 1987. However,  
204 analysis suggests there has been a reduction in fertilizer application rates per planted hectare, while area of planted corn has  
205 increased in recent decades (Wells et al., 2018). There was a likely trade-off in using this proxy; we were able to extend the period  
206 of record back to 1946, allowing for analysis of a wider range of lag times in the model, but might have sacrificed some accuracy  
207 in recent decades when nitrogen management may have improved. Lastly, vadose and saturated-zone transport rates were assumed  
208 to be constant over time (Wells et al., 2018).

## 209 2.5 Vadose and Saturated-zone Transport Rate Analysis

210 Ranges of vertical velocities (transport rates) through the vadose zone and saturated zone were estimated from  $^3\text{H}/^3\text{He}$   
211 age-dating in the Dutch Flats area in both 1998 (Verstraeten et al., 2001b) and 2016 (Wells et al., 2018) using Equation 2:

$$212 \quad V = \frac{R}{\theta}, \quad (2)$$

213 where  $R$  is the upper and lower bound of recharge rates (m/yr) indicated by groundwater ages, and  $\theta$  is mobile water content and  
214 porosity in the vadose and saturated zone, respectively. The use of  $^3\text{H}/^3\text{He}$  data was used in this study solely for constraining the  
215 range of transport rates to evaluate in the vadose and saturated zones, and as a base comparison to model results. The age-data,  
216 however, were not used by the model itself when seeking to identify an optimum transport rate combination. Throughout the text,  
217 unsaturated (vadose)-zone vertical transport rates will be abbreviated as  $V_u$ , while saturated-zone vertical transport rates will be  $V_s$ .  
218 In the vadose zone,  $\theta$  was assigned a constant value of 0.13, which was calibrated previously using a vertical transport model for  
219 the Dutch Flats area (Liao et al., 2012). In the saturated zone,  $\theta$  was assigned a constant value of 0.35, equal to the value assumed  
220 previously for recharge calculations (Böhlke et al., 2007). Vadose and saturated-zone travel times ( $\tau$ ) then were calculated using  
221 Equation 3:

$$222 \quad \tau = \frac{z}{V}, \quad (3)$$

223 where  $\tau$  is either vadose zone ( $\tau_u$ ) or saturated zone ( $\tau_s$ ) travel time in years, and  $z$  is the vadose-zone thickness ( $z_u$ ) or distance  
224 from the water table to well mid-screen ( $z_s$ ) in meters.



225            Though Equations 2 and 3 do not explicitly consider horizontal groundwater flow, they are believed to adequately model  
226 shallow groundwater ages, which are likely to follow approximately linear vertical age gradients near the water table. These simple  
227 equations are also suggested to sufficiently estimate groundwater age gradients in wedge-shaped aquifers (Cook and Böhlke, 2000),  
228 and Böhlke et al. (2007) found a linear model adequately fit their data in the Dutch Flats area. Nonetheless, saturated-zone transport  
229 rates and travel times calculated from Equations 2 and 3 should be considered “apparent” rates and travel times (i.e., similar to  
230 apparent groundwater ages, which are based on imperfect tracers). Additionally, it is emphasized that the assumed mobile water  
231 content of 0.13 is a calibrated parameter derived previously through inverse modelling and, as suggested by Liao et al. (2012), may  
232 have large uncertainties due to the varying site-specific characteristics known to exist from one well to the next.

233            Because of the influence of canal leakage on both intermediate and deep wells (Böhlke et al., 2007), only recharge rates  
234 from shallow wells were used to estimate vadose-zone travel times. The mean ( $\bar{x} = 0.38$  m/yr) and standard deviation ( $\sigma = \pm 0.23$   
235 m/yr) of all the 1998 ( $n=7$ ) and 2016 ( $n=2$ ) shallow recharge rates were calculated. Using  $\bar{x} \pm 1\sigma$ , a range of recharge rates from  
236 0.15 to 0.61 m/yr were converted to transport rates ( $V_u$ ) using Equation 2. This calculation resulted in 1.15 to 4.69 m/yr as the  
237 range of vadose-zone transport rates. Expanding the upper and lower bounds, a minimum vadose-zone transport rate of 1.0 m/yr  
238 and maximum of 4.75 m/yr was applied. Vertical transport rates in the vadose zone were increased by increments of 0.25 m/yr  
239 from 1.0 to 4.75 m/yr, resulting in 16 possible vadose-zone transport rates to evaluate in the Random Forest model.

240            Mean ( $\bar{x} = 0.84$  m/yr) and standard deviation ( $\sigma = \pm 0.73$  m/yr) of all shallow, intermediate, and deep well recharge rates  
241 were included in identifying a range of saturated-zone recharge rates from 0.10 to 1.57 m/yr. A total of 35 and 8 recharge rates  
242 were used from the 1990s and Wells et al. (2018) studies, respectively. Equation 2 was used to calculate saturated-zone transport  
243 rates ( $V_s$ ) of 0.28 and 4.49 m/yr. Saturated zone transport rates were increased by increments of 0.25 m/yr, from 0.25 to 4.5 m/yr,  
244 resulting in 18 unique saturated-zone transport rates to evaluate in the Random Forest model. The range of transport rates suggested  
245 by groundwater age-dating was large (more than an order of magnitude) and would be considered to include rates likely to be  
246 expected in a variety of field settings. Presumably, the same model constraints and results could have been obtained without the  
247 prior age data and with some relatively conservative estimates.

248            Travel times  $\tau_u$  and  $\tau_s$  were calculated for each well based on  $z_u$  and  $z_s$ , respectively. For every possible combination of  
249 vadose and saturated-zone transport rates, a unique total travel time,  $\tau_t$ , was calculated for each well based on the vadose and  
250 saturated-zone dimensions of that particular well.

$$251 \quad \tau_t = \tau_u + \tau_s, \quad (4)$$

252            The total travel times from Equation 4 were used to lag dynamic predictors relative to each nitrate sample date. For  
253 instance, a nitrate sample collected in 2010 at a well with a 20-year total travel time (e.g.,  $\tau_u = 10$  yrs and  $\tau_s = 10$  yrs) would be  
254 assigned the 1990 values for precipitation (450 mm), Interstate Canal discharge (0.4 km<sup>3</sup>/yr), center pivot irrigated area (2484  
255 hectares), and area of planted corn (8905 hectares).

256            A total of 288 unique transport rate combinations (corresponding to different combinations of the 16 vadose and 18  
257 saturated-zone transport rates) were joined into a single dataset totalling over 300,000 observations to determine the optimal rate  
258 resulting in the maximum testing NSE from the model. Each transport rate combination incorporated up to 1,049 groundwater  
259 [NO<sub>3</sub><sup>-</sup>] values. To decrease runtime, Random Forest models were parallel processed through a Holland Computing Center (HCC)  
260 cluster at the University of Nebraska-Lincoln.



## 261 **3 Results and Discussion**

262 This study addressed a relatively unexplored use of Random Forest, which was to identify optimal lag times based on  
263 testing a range of transport rate combinations through the vadose and saturated zones, historical nitrate concentrations, and the use  
264 of easily accessible environmental datasets.

### 265 **3.1. Relative Importance of Transport Time and Dynamic Variables**

266 In our initial modelling with dynamic predictors, we anticipated that we could use the Random Forest model with the  
267 highest NSE to identify the optimal pair of vadose and saturated-zone transport rates. However, no clear pattern emerged among  
268 the different models (Fig. 3). Given the small differences and lack of defined pattern in testing NSE values, we selected ten transport  
269 rate combinations (the five top performing models, plus four transport rate combinations of high and low transport rates, and one  
270 intermediate transport rate combination) for further evaluation of variable importance and sensitivity to a range of transport rate  
271 combinations (Table 2). Median total travel time ranked third in variable importance, while the four dynamic variables consistently  
272 had the four lowest rankings (Fig. 4). Total travel time also had the greatest variability in importance among the fifteen variables,  
273 with a range of 18.4% between the upper and lower values, suggesting some model sensitivity to lag times. Excluding total travel  
274 time, the remaining variables had an average variable importance range of 6%.

275 Dynamic variables had little influence on the model, despite common potential linkages to groundwater [ $\text{NO}_3^-$ ] (Böhlke  
276 et al., 2007; Exner et al., 2010; Spalding et al., 2001). A pattern emerged among dynamic variables where the stronger the historical  
277 trend of the predictor, the greater the importance of the predictor (Fig. 2; Fig.4). For instance, center pivot irrigated area (highest  
278 ranking dynamic variable) had the least noise and the most pronounced trend, while annual precipitation (lowest ranking variable)  
279 was highly variable and lacked any trend over time (Fig. 2), and also may not be a substantial source of recharge (Böhlke et al.,  
280 2007). Further exploration could be done to test more refined variables – for instance, annual median rainfall intensity for the  
281 growing season might have a more direct connection to nitrate leaching than total annual precipitation. However, rainfall intensity  
282 data are not readily available. Dynamic variables could be of more use in other study areas that undergo relatively rapid and  
283 pronounced changes (e.g., land use). In future work, the model sensitivity to dynamic variables could be tested through formal  
284 sensitivity analysis and/or automated variable selection algorithms (Eibe et al., 2016).

285 Ultimately, results from initial analyses suggest that (1) the dynamic data did little to improve model performance, and  
286 (2) Random Forest was not able to relate the four considered dynamic predictors to [ $\text{NO}_3^-$ ] in a meaningful way that could be used  
287 to estimate lag time. It has also been suggested by Katz et al. (2001) that a monotonic trend in an independent variable is not  
288 necessarily linearly related to the dependent variable. It is likely the influence of these dynamic predictors are dampened as nitrate  
289 is transported from the surface to wells such that data-driven approaches are unable to sort through noise to identify relationships.

### 290 **3.2 Use of Random Forest to determine transport rates**

291 Due to their low relative importance as predictors, all four dynamic predictors were removed in the subsequent analysis. As  
292 discussed above, a notable variation in total travel time  $\%_{\text{inc}}\text{MSE}$  was observed in Fig. 4, suggesting model sensitivity to this  
293 variable. Additionally, a relationship between travel time and [ $\text{NO}_3^-$ ] has been suggested in the Dutch Flats area through previous  
294 studies (Böhlke et al., 2007; Wells et al., 2018). Therefore, a second analysis of just the 11 static predictors was performed over  
295 the full range of vadose and saturated transport rates (i.e., 288 combinations). However, in the second analysis, model sensitivity  
296 to total travel time – evaluated with respect to the transport rate combination corresponding to the largest  $\%_{\text{inc}}\text{MSE}$  of total travel  
297 time – was used to determine a distinguished transport rate combination.



298 The Random Forest models were useful in identifying the relative magnitudes of  $V_u$  and  $V_s$  that led to high %<sub>inc</sub>MSE.  
299 Based on the heat map of %<sub>inc</sub>MSE, a band of transport rate combinations with consistently high %<sub>inc</sub>MSE was visually apparent  
300 (Fig. 5). The upper and lower bounds of the band translate to transport rate ratios ( $V_s/V_u$ ) ranging from 0.9 to 1.5, and are values  
301 that could be useful in constraining recharge and/or transport rate estimates in more complex mechanistic models, as part of a  
302 hybrid modelling approach. This is especially important since recharge is one of the most sensitive parameters in a groundwater  
303 model (Mittelstet et al., 2011), yet one with high uncertainty.

304 The %<sub>inc</sub>MSE of total travel time in the second analysis ranged from 20.6 to 31.5%, with the largest %<sub>inc</sub>MSE associated  
305 with vadose and saturated-zone transport rates of 3.50 m/yr and 3.75 m/yr, respectively (Fig. 5), and the top four predictors for this  
306 transport rate combination were total travel time, vadose-zone thickness, dissolved oxygen, and saturated thickness (Fig. 6).  
307 Converting those vadose and saturated-zone transport rates to recharge rates yielded values of 0.46 m/yr and 1.31 m/yr,  
308 respectively. Such a large difference between the two recharge values would be unexpected in most unconsolidated surficial (water-  
309 table) aquifers receiving diffuse recharge, but it is consistent with the hydrologic conceptual model of the Dutch Flats area. In fact,  
310 both model recharge rates compare favourably with recharge rates calculated from the previous Dutch Flats studies using  $^3\text{H}/^3\text{He}$   
311 age-dating (Böhlke et al., 2007; Wells et al., 2018). For instance, the recharge rate determined from the vadose-zone transport rate  
312 in this study (0.46 m/yr) was comparable to the mean recharge rate of 0.38 m/yr ( $n = 9$ ) from groundwater age-dating at shallow  
313 wells, which are most representative of diffuse recharge below crop fields. Additionally, the recharge rate (1.31 m/yr) determined  
314 from the saturated-zone transport rate was consistent with the mean recharge value derived from groundwater ages in intermediate  
315 wells (1.22 m/yr,  $n = 13$ ). Intermediate wells are variably impacted by focused recharge from canals in upgradient areas. Given the  
316 similarity in diffuse recharge and focused recharge estimates from both Random Forest and groundwater age-dating, the transport  
317 rate ratios (1.2 and 1.1, respectively) were consistent. That is, the Random Forest modelling framework produced transport rates  
318 consistent with the major hydrological processes in Dutch Flats both in direct (i.e., transport rate estimates) and relative (i.e.,  
319 transport rate ratio) terms.

320 Assuming the Random Forest approach has accurately captured the two major recharge processes (diffuse recharge over  
321 crop fields and focused recharge from canals), a comparison of recharge rates from all sampled groundwater wells representative  
322 of recharge to the groundwater system as a whole (0.84 m/yr,  $n = 43$ ) to the recharge rates from Random Forest modelling (0.46  
323 and 1.31 m/yr) would provide an estimate of the relative importance of diffuse versus focused recharge on overall recharge in  
324 Dutch Flats. Under these assumptions, diffuse recharge would account for approximately 55%, while focused recharge would  
325 account for about 45% of total recharge in the Dutch Flats area. Similarly, Böhlke et al. (2007) concluded that these two recharge  
326 sources contributed roughly equally to the aquifer on the basis of groundwater age profiles, as well as from dissolved atmospheric  
327 gas data indicating mean recharge temperatures between those expected of diffuse infiltration and focused canal leakage.

328 Partial dependence plots, which illustrate the impact a single predictor has on  $[\text{NO}_3^-]$  in the model with respect to other  
329 predictors (Fig. 7), largely reflect the conceptual understanding of the system from previous studies including Böhlke et al. (2007)  
330 and Wells et al. (2018). Key features that strengthen confidence in the Random Forest modelling include (1) depth to bottom  
331 screen, where groundwater  $[\text{NO}_3^-]$  is lower at greater depths, (2) the effects of minor and major canals, where groundwater  $[\text{NO}_3^-]$   
332 in the vicinity of canals is diluted by canal leakage, and the influence of major canals extends further from the canal, (3) land  
333 surface elevation, where elevations indicating proximity to major canals are associated with relatively lower groundwater  $[\text{NO}_3^-]$ ,  
334 and (4) DO concentration, where higher DO concentration is linked to higher groundwater  $[\text{NO}_3^-]$ . We note that decreasing DO  
335 and  $[\text{NO}_3^-]$  with groundwater age can be explained by DO reduction and historical changes in  $[\text{NO}_3^-]$  recharge, whereas  
336 groundwater chemistry and nitrate isotopic data recorded in both this study and previous Dutch Flats studies suggest nitrate  
337 reduction was not a major factor in this alluvial aquifer.



338 The partial dependence plot for total travel time exhibits a pronounced threshold, where  $[\text{NO}_3^-]$  is markedly higher for  
339 groundwater with travel time less than seven years. It is possible this reflects long-term stratification of distinct groundwater  $[\text{NO}_3^-]$   
340 ], stemming from the suggested patterns stated above as it relates to aquifer depth and the influences of diffuse and focused recharge  
341 in the region. This seven-year threshold is lower than a previous estimate of mean groundwater age alone (8.8 years; where  
342 groundwater age neglects vadose-zone travel time) and suggests that rapid aquifer response to changes in nitrogen management in  
343 Dutch Flats is possible.

### 344 **3.3 Opportunities and limitations of Random Forest approach in estimating lag times**

345 Overall, results suggest that in a complex system such as Dutch Flats, Random Forest was able to identify reasonable  
346 transport rates for both the vadose and saturated zones, and with additional validation, this method may offer an inexpensive (i.e.,  
347 compared to groundwater age-dating across a large monitoring well network and/or complex modelling) and reasonable technique  
348 for estimating lag time from historical monitoring data. Further, this approach allows for additional insight on groundwater  
349 dynamics to be extracted from existing monitoring data. However, this study was conducted in the context of a larger project  
350 (Wells et al., 2018) and built on prior research on groundwater flow and nitrate concentrations in the study area (Böhlke et al.,  
351 2007). Therefore, it is critical in future work to consider the “black box” nature of statistical machine learning approach, as  
352 highlighted in key considerations below.

353

354 Some key considerations for future application of this approach include:

- 355 (1) The Random Forest approach might be useful for estimating future recharge and  $[\text{NO}_3^-]$  using multiple potential  
356 management scenarios, as long as considered management scenarios fall within the range of historical observations used  
357 to train the model. This information could be used to inform policy makers of the impact that current and future  
358 management decisions will have on recharge and  $[\text{NO}_3^-]$ .
- 359 (2) The Dutch Flats overlies a predominantly oxic aquifer, where nitrate transport is mostly conservative. In aquifers with  
360 both oxic and anoxic conditions and distinct nitrate extinction depths (Liao et al., 2012; Welch et al., 2011), this approach  
361 may be biased toward oxic portions of the aquifer where the nitrate signal is preserved.
- 362 (3) While estimates of vadose and saturated-zone transport rates determined from  $\%_{\text{inc}}\text{MSE}$  are consistent with previous  
363 studies, the predictive performance of the selected model (based on NSE and visual inspection of predicted versus  
364 observed nitrate plots) was not substantially different than other models tested. In other words, the “optimal model” was  
365 non-unique in terms of predicting  $[\text{NO}_3^-]$ . Testing the approach of using  $\%_{\text{inc}}\text{MSE}$  in other vadose and saturated zones,  
366 with substantial comparison to previous transport rate estimates, is warranted.
- 367 (4) Despite potential non-uniqueness in prediction metrics, the heat map of  $\%_{\text{inc}}\text{MSE}$  did reveal an orderly pattern suggesting  
368 consistent transport rate ratios. For modelling efforts where recharge rates are a key calibration parameter, identification  
369 of a range of reasonable recharge rates, and/or the ratio of recharge rates from diffuse and focused recharge sources for a  
370 complex system will reduce model uncertainty and improve results. This statistical machine learning approach, which  
371 essentially leverages nitrate as a tracer, may provide valuable insight to complement relatively expensive groundwater  
372 age-dating or vadose-zone monitoring data, or as a standalone approach for first-order approximations.
- 373 (5) The demonstrated statistical machine learning approach is apparently well-suited for drawing out transport rate  
374 information from a site with two distinct recharge sources (diffuse versus focused recharge sources) driving the  
375 groundwater nitrate dynamics. Further testing is needed at sites where recharge and nitrate dynamics are more subtle.



#### 376 4 Conclusions

377 The Dutch Flats area consists of large variations in  $[\text{NO}_3^-]$  throughout a relatively small region in western Nebraska. Long-  
378 term groundwater  $[\text{NO}_3^-]$  and previous groundwater age-dating studies in Dutch Flats provided an opportune setting to test a new  
379 application of statistical machine learning (Random Forest) for determining vadose and saturated-zone transport rates. Overall  
380 results suggest Random Forest has the capability to both identify reasonable transport rates (and lag time) and key variables  
381 influencing groundwater  $[\text{NO}_3^-]$ , albeit with potential for non-unique results. Limitations were also identified when using dynamic  
382 predictors to model groundwater  $[\text{NO}_3^-]$ . Utilizing only static predictors, and Random Forest's ability to evaluate variable  
383 importance, a vadose and saturated-zone transport rate was selected based on model sensitivity to changing the total travel time  
384 predictor. In other words, total travel time variable importance was evaluated for 288 different transport rate combinations, and the  
385 combination with a total travel time having the largest influence over the model's ability to predict  $[\text{NO}_3^-]$  was selected for  
386 additional examination. This analysis identified a vadose and saturated-zone transport rate combination consistent with rates  
387 previously estimated from  $^3\text{H}/^3\text{He}$  age-dating in Böhlke et al. (2007) and Wells et al. (2018), in both direct and relative terms.

388 Future studies should include assessments of the proper conditions for application of dynamic predictors and include  
389 comparisons of data-driven analyses with complementary datasets. Despite noted limitations, partial dependence plots and relative  
390 importance of predictors were largely consistent with previous findings and mechanistic understanding of the study area, giving  
391 greater confidence in model outputs. The influence of canal leakage on groundwater recharge rates and  $[\text{NO}_3^-]$ , for example, was  
392 consistent with previous Dutch Flats studies. Partial dependence plots suggest a threshold of higher  $[\text{NO}_3^-]$  for groundwater with  
393 total travel time (vadose and saturated-zone travel times, combined) of less than seven years, indicating the potential for relatively  
394 rapid groundwater  $[\text{NO}_3^-]$  response to widespread implementation of best management practices.

395

396 **Author contribution:** TG, AM, and NN were responsible for conceptualization. MW and NN developed the model code and MW  
397 performed formal analysis. MW prepared the manuscript from his M.S. thesis with contributions from all co-authors. TG was  
398 responsible for project administration and funding acquisition.

399

400 **Acknowledgements:** The authors acknowledge the North Platte Natural Resources District for providing technical assistance and  
401 resources, including long-term groundwater nitrate data accessed via the Quality-Assessed Agrichemical Contaminant Database  
402 for Nebraska Groundwater. We also thank Steve Sibray and Mason Johnson for their support in field sampling efforts.

403

404 **Funding:** This work was supported by the U.S. Geological Survey 104b Program (Project 2016NE286B), U.S. Department of  
405 Agriculture—National Institute of Food and Agriculture NEB-21-177 (Hatch Project 1015698), and Daugherty Water for Food  
406 Global Institute Graduate Student Fellowship.

407

408 **Code and Data Availability:** Code is available on request. Data used in the random forest model and described in the supplemental  
409 information is available via the University of Nebraska – Lincoln Data Repository (<https://doi.org/10.32873/unl.dr.20200428>).

#### 410 References

411 Anning, D. W., Paul, A. P., McKinney, T. S., Huntington, J. M., Bexfield, L. M. and Thiros, S. A.: Predicted nitrate and arsenic  
412 concentrations in basin-fill aquifers of the Southwestern United States, Report, United States Geological Survey. [online] Available  
413 from: <https://pubs.usgs.gov/sir/2012/5065/>, 2012.



- 414 Babcock, H. M., Visher, F. N. and Durum, W. H.: Ground-water conditions in the Dutch Flats area, Scotts Bluff and Sioux  
415 Counties, Nebraska, with a section on chemical quality of the ground water, Report. [online] Available from:  
416 <http://pubs.er.usgs.gov/publication/cir126>, 1951.
- 417 Ball, L. B., Kress, W. H., Steele, G. V., Cannia, J. C. and Andersen, M. J.: Determination of canal leakage potential using  
418 continuous resistivity profiling techniques, Interstate and Tri-State Canals, western Nebraska and eastern Wyoming, 2004, Report,  
419 United States Geological Survey. [online] Available from: <http://pubs.er.usgs.gov/publication/sir20065032>, 2006.
- 420 Böhlke, J. K.: Groundwater recharge and agricultural contamination, *Hydrogeology Journal*, 10(1), 153–179, doi:10.1007/s10040-  
421 001-0183-3, 2002.
- 422 Böhlke, J. K. and Denver, J. M.: Combined Use of Groundwater Dating, Chemical, and Isotopic Analyses to Resolve the History  
423 and Fate of Nitrate Contamination in Two Agricultural Watersheds, Atlantic Coastal Plain, Maryland, *Water Resources Research*,  
424 31(9), 2319–2339, doi:10.1029/95WR01584, 1995.
- 425 Böhlke, J. K., Wanty, R., Tuttle, M., Delin, G. and Landon, M.: Denitrification in the recharge area and discharge area of a transient  
426 agricultural nitrate plume in a glacial outwash sand aquifer, Minnesota: Denitrification in recharge and discharge areas, *Water*  
427 *Resources Research*, 38(7), 10-1-10–26, doi:10.1029/2001WR000663, 2002.
- 428 Böhlke, J. K., Verstraeten, I. M. and Kraemer, T. F.: Effects of surface-water irrigation on sources, fluxes, and residence times of  
429 water, nitrate, and uranium in an alluvial aquifer, *Applied Geochemistry*, 22(1), 152–174, doi:10.1016/j.apgeochem.2006.08.019,  
430 2007.
- 431 Breiman, L.: Random Forests, *Machine Learning*, 45(1), 5–32, doi:10.1023/A:1010933404324, 2001.
- 432 Browne, B. A. and Guldán, N. M.: Understanding Long-Term Baseflow Water Quality Trends Using a Synoptic Survey of the  
433 Ground Water–Surface Water Interface, Central Wisconsin, *Journal of Environment Quality*, 34(3), 825,  
434 doi:10.2134/jeq2004.0134, 2005.
- 435 Cherry, M., Gilmore, T., Mittelstet, A., Gastmans, D., Santos, V. and Gates, J. B.: Recharge seasonality based on stable isotopes:  
436 Nongrowing season bias altered by irrigation in Nebraska, *Hydrological Processes*, doi:10.1002/hyp.13683, 2020.
- 437 Cook, P. G. and Böhlke, J. K.: Determining Timescales for Groundwater Flow and Solute Transport, in *Environmental Tracers in*  
438 *Subsurface Hydrology*, edited by P. G. Cook and A. L. Herczeg, pp. 1–30, Springer US, Boston, MA., 2000.
- 439 Dieter, C. A., Maupin, M. A., Caldwell, R. R., Harris, M. A., Ivahnenko, T. I., Lovelace, J. K., Barber, N. L. and Linsey, K. S.:  
440 Estimated use of water in the United States in 2015, Report, Reston, VA., 2018.
- 441 Eberts, S. M., Thomas, M. S. and Jagucki, M. L.: The quality of our Nation’s waters—Factors affecting public-supply-well  
442 vulnerability to contamination—Understanding observed water quality and anticipating future water quality, U.S. Geological  
443 Survey Circular 1385. [online] Available from: <https://pubs.usgs.gov/circ/1385/>, 2013.
- 444 Efron, B.: Bootstrap Methods: Another Look at the Jackknife, *The Annals of Statistics*, 7(1), 1–26, doi:10.1214/aos/1176344552,  
445 1979.
- 446 Eibe, F., Hall, M. A. and Witten, I. H.: The WEKA Workbench, in Online Appendix for “Data Mining: Practical Machine Learning  
447 Tools and Techniques,” Morgan Kaufmann., 2016.
- 448 Exner, M. E., Perea-Estrada, H. and Spalding, R. F.: Long-Term Response of Groundwater Nitrate Concentrations to Management  
449 Regulations in Nebraska’s Central Platte Valley, *The Scientific World Journal*, 10, 286–297, doi:10.1100/tsw.2010.25, 2010.
- 450 Gilmore, T. E., Genereux, D. P., Solomon, D. K. and Solder, J. E.: Groundwater transit time distribution and mean from streambed  
451 sampling in an agricultural coastal plain watershed, North Carolina, USA: Groundwater transit time, *Water Resources Research*,  
452 52(3), 2025–2044, doi:10.1002/2015WR017600, 2016.
- 453 Green, C. T., Liao, L., Nolan, B. T., Juckem, P. F., Shope, C. L., Tesoriero, A. J. and Jurgens, B. C.: Regional Variability of Nitrate  
454 Fluxes in the Unsaturated Zone and Groundwater, Wisconsin, USA, *Water Resources Research*, 54(1), 301–322,  
455 doi:10.1002/2017WR022012, 2018.



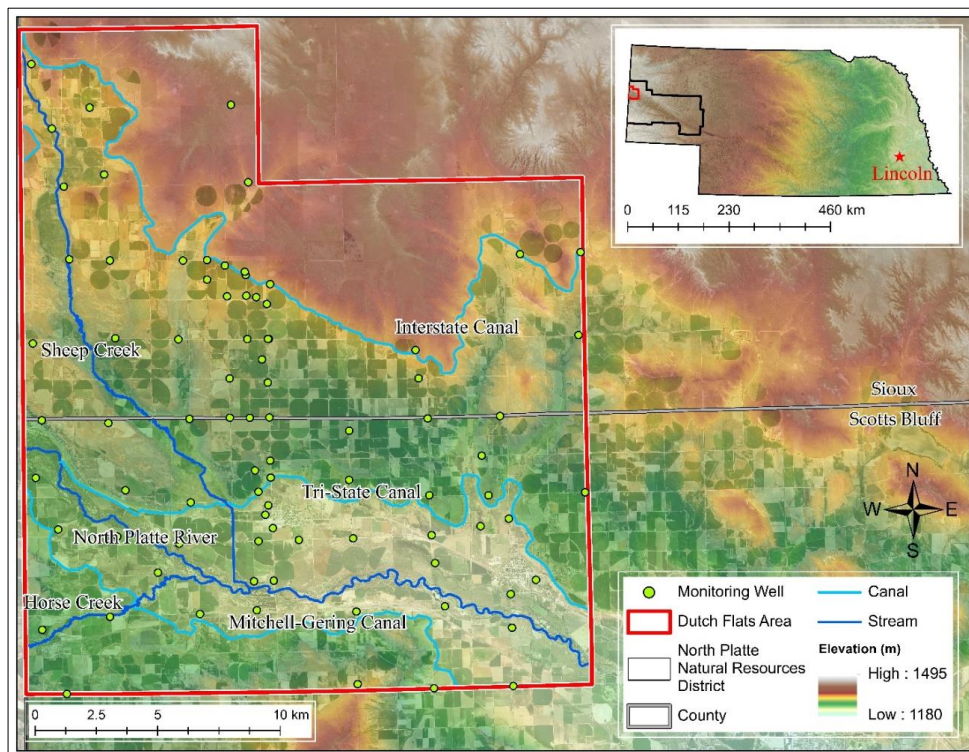
- 456 Harvey, F. E. and Sibray, S. S.: Delineating Ground Water Recharge from Leaking Irrigation Canals Using Water Chemistry and  
457 Isotopes, *Ground Water*, 39(3), 408–421, doi:10.1111/j.1745-6584.2001.tb02325.x, 2001.
- 458 Hastie, T., Tibshirani, R. and Friedman, J. H.: *The elements of statistical learning: data mining, inference, and prediction*, 2nd ed.,  
459 Springer, New York, NY., 2009.
- 460 Hobza, C. M. and Andersen, M. J.: Quantifying canal leakage rates using a mass-balance approach and heat-based hydraulic  
461 conductivity estimates in selected irrigation canals, western Nebraska, 2007 through 2009, Report, United States Geological  
462 Survey. [online] Available from: <http://pubs.er.usgs.gov/publication/sir20105226>, 2010.
- 463 Homer, C. G., Dewitz, J., Yang, L., Jin, S., Danielson, P., Xian, G. Z., Coulston, J., Herold, N., Wickham, J. and Megown, K.:  
464 Completion of the 2011 National Land Cover Database for the conterminous United States – Representing a decade of land cover  
465 change information, *Photogrammetric Engineering and Remote Sensing*, 81, 345354, 2015.
- 466 Hudson, C. (NPNRD): Personal Communication with M.J. Wells, University of Nebraska, Lincoln, NE, USA, 2018.
- 467 Ilampooranan, I., Van Meter, K. J. and Basu, N. B.: A Race against Time: Modelling Time Lags in Watershed Response, *Water*  
468 *Resources Research*, doi:10.1029/2018WR023815, 2019.
- 469 Irmak, S., Odhiambo, L., Kranz, W. L. and Eisenhauer, D. E.: Irrigation Efficiency And Uniformity, And Crop Water Use  
470 Efficiency, Extension Circular, University of Nebraska – Lincoln, Lincoln, NE. [online] Available from: Available at  
471 <http://extensionpubs.unl.edu/>, 2011.
- 472 Jones, Z. M. and Linder, F. J.: Exploratory Data Analysis using Random Forests, in 73rd Annual MPSA Conference, pp. 1–31.  
473 [online] Available from: [http://zmjones.com/static/papers/rfss\\_manuscript.pdf](http://zmjones.com/static/papers/rfss_manuscript.pdf) (Accessed 25 May 2018), 2015.
- 474 Katz, B. G., Böhlke, J. K. and Hornsby, H. D.: Timescales for nitrate contamination of spring waters, northern Florida, USA,  
475 *Chemical Geology*, 179(1–4), 167–186, doi:10.1016/S0009-2541(01)00321-7, 2001.
- 476 Kennedy, C. D., Genereux, D. P., Corbett, D. R. and Mitsova, H.: Spatial and temporal dynamics of coupled groundwater and  
477 nitrogen fluxes through a streambed in an agricultural watershed: Groundwater and nitrogen fluxes in a streambed, *Water*  
478 *Resources Research*, 45(9), doi:10.1029/2008WR007397, 2009.
- 479 Kuhn, M.: Building Predictive Models in *R* Using the caret Package, *Journal of Statistical Software*, 28(5),  
480 doi:10.18637/jss.v028.i05, 2008.
- 481 Liao, L., Green, C. T., Bekins, B. A. and Böhlke, J. K.: Factors controlling nitrate fluxes in groundwater in agricultural areas:  
482 Factors controlling nitrate fluxes in groundwater, *Water Resources Research*, 48(6), doi:10.1029/2011WR011008, 2012.
- 483 Luckey, R. R. and Cannia, J. C.: Groundwater Flow Model of the Western Model Unit of the Nebraska Cooperative Hydrology  
484 Study (COHYST) Area, Nebraska Department of Natural Resources, Lincoln, NE. [online] Available from:  
485 [ftp://ftp.dnr.nebraska.gov/Pub/cohystftp/cohyst/model\\_reports/WMU\\_Documentation\\_060519.pdf](ftp://ftp.dnr.nebraska.gov/Pub/cohystftp/cohyst/model_reports/WMU_Documentation_060519.pdf), 2006.
- 486 McMahon, P. B., Dennehy, K. F., Bruce, B. W., Böhlke, J. K., Michel, R. L., Gurdak, J. J. and Hurlbut, D. B.: Storage and transit  
487 time of chemicals in thick unsaturated zones under rangeland and irrigated cropland, High Plains, United States: Chemical storage  
488 in thick unsaturated zone, *Water Resources Research*, 42(3), doi:10.1029/2005WR004417, 2006.
- 489 Meals, D. W., Dressing, S. A. and Davenport, T. E.: Lag Time in Water Quality Response to Best Management Practices: A  
490 Review, *Journal of Environment Quality*, 39(1), 85, doi:10.2134/jeq2009.0108, 2010.
- 491 Mittelstet, A. R., Smolen, M. D., Fox, G. A. and Adams, D. C.: Comparison of Aquifer Sustainability Under Groundwater  
492 Administrations in Oklahoma and Texas: Comparison of Aquifer Sustainability Under Groundwater Administrations in Oklahoma  
493 and Texas, *JAWRA Journal of the American Water Resources Association*, 47(2), 424–431, doi:10.1111/j.1752-  
494 1688.2011.00524.x, 2011.
- 495 Morgenstern, U., Daughney, C. J., Leonard, G., Gordon, D., Donath, F. M. and Reeves, R.: Using groundwater age and  
496 hydrochemistry to understand sources and dynamics of nutrient contamination through the catchment into Lake Rotorua, New  
497 Zealand, *Hydrology and Earth System Sciences*, 19(2), 803–822, doi:10.5194/hess-19-803-2015, 2015.



- 498 Nash, J. E. and Sutcliffe, J. V.: River flow forecasting through conceptual models part I — A discussion of principles, *Journal of*  
499 *Hydrology*, 10(3), 282–290, doi:10.1016/0022-1694(70)90255-6, 1970.
- 500 NASS: USDA/NASS QuickStats Ad-hoc Query Tool, [online] Available from: <https://quickstats.nass.usda.gov/> (Accessed 15  
501 February 2018), 2018.
- 502 NEDNR: 7.5 Digital Elevation Models, Elevation Data [online] Available from: <https://dnr.nebraska.gov/data/elevation-data>,  
503 1997.
- 504 NEDNR: Fifty-fifth biennial report of the Department of Natural Resources, Nebraska Department of Natural Resources, Lincoln,  
505 NE. [online] Available from: [https://dnr.nebraska.gov/sites/dnr.nebraska.gov/files/doc/surface-water/biennial-](https://dnr.nebraska.gov/sites/dnr.nebraska.gov/files/doc/surface-water/biennial-reports/BiennialReport2005-06.pdf)  
506 [reports/BiennialReport2005-06.pdf](https://dnr.nebraska.gov/sites/dnr.nebraska.gov/files/doc/surface-water/biennial-reports/BiennialReport2005-06.pdf), 2009.
- 507 Nelson, N. G., Muñoz-Carpena, R., Philips, E. J., Kaplan, D., Sucsy, P. and Hendrickson, J.: Revealing Biotic and Abiotic Controls  
508 of Harmful Algal Blooms in a Shallow Subtropical Lake through Statistical Machine Learning, *Environmental Science &*  
509 *Technology*, 52(6), 3527–3535, doi:10.1021/acs.est.7b05884, 2018.
- 510 NOAA: National Climatic Data Center (NCDC), [online] Available from: <https://www.ncdc.noaa.gov/cdo-web/datatools>  
511 (Accessed 4 August 2017), 2017.
- 512 Nolan, B. T., Gronberg, J. M., Faunt, C. C., Eberts, S. M. and Belitz, K.: Modeling Nitrate at Domestic and Public-Supply Well  
513 Depths in the Central Valley, California, *Environmental Science & Technology*, 48(10), 5643–5651, doi:10.1021/es405452q,  
514 2014.
- 515 Nolan, B. T., Green, C. T., Juckem, P. F., Liao, L. and Reddy, J. E.: Metamodeling and mapping of nitrate flux in the unsaturated  
516 zone and groundwater, Wisconsin, USA, *Journal of Hydrology*, 559, 428–441, doi:10.1016/j.jhydrol.2018.02.029, 2018.
- 517 NRCS: Web Soil Survey. [online] Available from: <https://websoilsurvey.sc.egov.usda.gov/> (Accessed 16 November 2017), 2018.
- 518 Ouedraogo, I., Defourny, P. and Vanclooster, M.: Validating a continental-scale groundwater diffuse pollution model using  
519 regional datasets, *Environmental Science and Pollution Research*, doi:10.1007/s11356-017-0899-9, 2017.
- 520 Preston, T. (NPNRD): Personal Communication with M.J. Wells, University of Nebraska, Lincoln, NE, USA, 2017.
- 521 Puckett, L. J., Tesoriero, A. J. and Dubrovsky, N. M.: Nitrogen Contamination of Surficial Aquifers—A Growing Legacy †,  
522 *Environmental Science & Technology*, 45(3), 839–844, doi:10.1021/es1038358, 2011.
- 523 R Core Team: R: A language and environment for statistical computing, R Foundation for Statistical Computing, Vienna, Austria.  
524 [online] Available from: <https://www.R-project.org/>, 2017.
- 525 Ransom, K. M., Nolan, B. T., A. Traum, J., Faunt, C. C., Bell, A. M., Gronberg, J. A. M., Wheeler, D. C., Z. Rosecrans, C.,  
526 Jurgens, B., Schwarz, G. E., Belitz, K., M. Eberts, S., Kourakos, G. and Harter, T.: A hybrid machine learning model to predict  
527 and visualize nitrate concentration throughout the Central Valley aquifer, California, USA, *Science of The Total Environment*,  
528 601–602, 1160–1172, doi:10.1016/j.scitotenv.2017.05.192, 2017.
- 529 Rodriguez-Galiano, V. F., Mendes, M. P., Garcia-Soldado, M. J., Chica-Olmo, M. and Ribeiro, L.: Predictive modeling of  
530 groundwater nitrate pollution using Random Forest and multisource variables related to intrinsic and specific vulnerability: A case  
531 study in an agricultural setting (Southern Spain), *Science of The Total Environment*, 476–477, 189–206,  
532 doi:10.1016/j.scitotenv.2014.01.001, 2014.
- 533 Rossman, N. R., Zlotnik, V. A., Rowe, C. M. and Szilagyi, J.: Vadose zone lag time and potential 21st century climate change  
534 effects on spatially distributed groundwater recharge in the semi-arid Nebraska Sand Hills, *Journal of Hydrology*, 519, 656–669,  
535 doi:10.1016/j.jhydrol.2014.07.057, 2014.
- 536 Russoniello, C. J., Konikow, L. F., Kroeger, K. D., Fernandez, C., Andres, A. S. and Michael, H. A.: Hydrogeologic controls on  
537 groundwater discharge and nitrogen loads in a coastal watershed, *Journal of Hydrology*, 538, 783–793,  
538 doi:10.1016/j.jhydrol.2016.05.013, 2016.



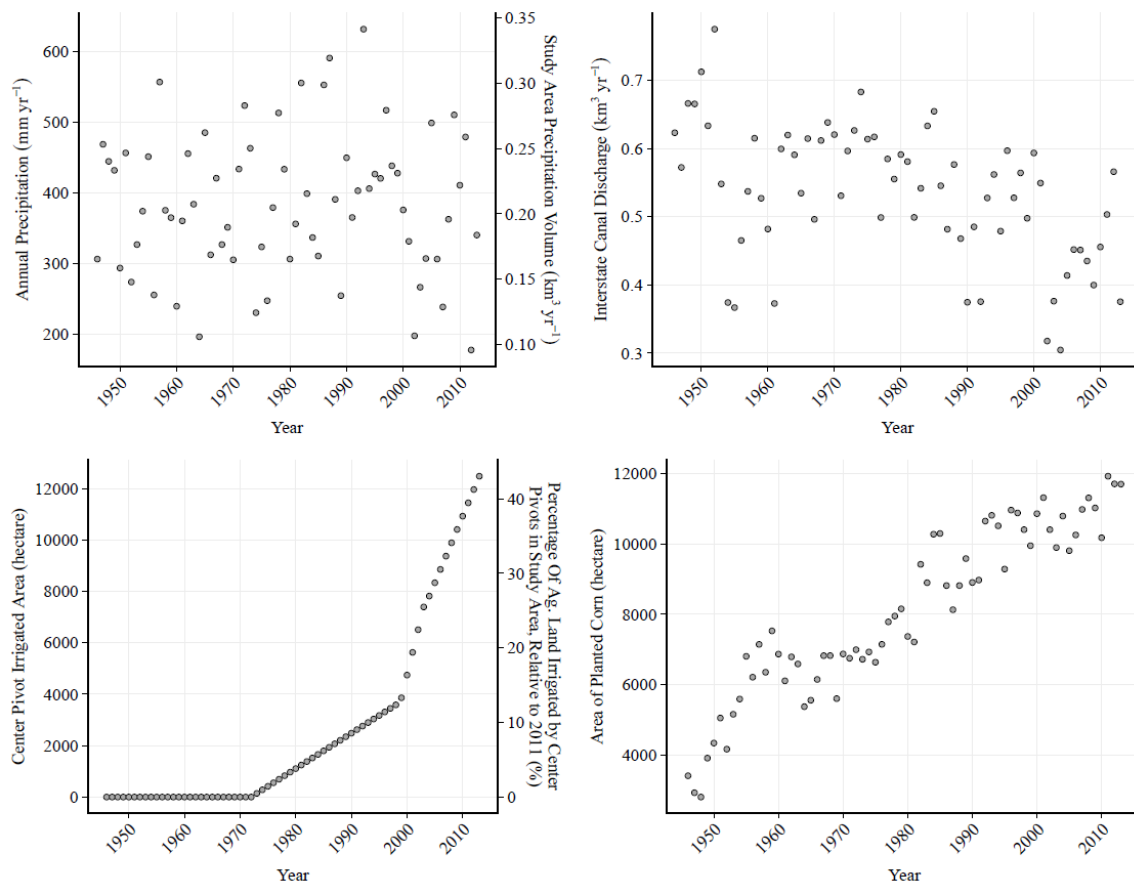
- 539 Spalding, R. F., Watts, D. G., Schepers, J. S., Burbach, M. E., Exner, M. E., Poreda, R. J. and Martin, G. E.: Controlling Nitrate  
540 Leaching in Irrigated Agriculture, *Journal of Environment Quality*, 30(4), 1184, doi:10.2134/jeq2001.3041184x, 2001.
- 541 Turkeltaub, T., Kurtzman, D. and Dahan, O.: Real-time monitoring of nitrate transport in the deep vadose zone under a crop field  
542 – implications for groundwater protection, *Hydrology and Earth System Sciences*, 20(8), 3099–3108, doi:10.5194/hess-20-3099-  
543 2016, 2016.
- 544 University of Nebraska-Lincoln: Quality-Assessed Agrichemical Contaminant Database for Nebraska Ground Water, [online]  
545 Available from: <https://clearinghouse.nebraska.gov/Clearinghouse.aspx> (Accessed 5 September 2016), 2016.
- 546 USBR: Hydromet: Archive Data Access, [online] Available from: [https://www.usbr.gov/gp/hydromet/hydromet\\_arcread.html](https://www.usbr.gov/gp/hydromet/hydromet_arcread.html)  
547 (Accessed 22 May 2018), 2018.
- 548 USDA: NAIP and NAPP Imagery, [online] Available from <https://dnr.nebraska.gov/data/digital-imagery> (Accessed 14 August  
549 2017), 2017.
- 550 USGS: LANDSAT Imagery, [online] Available from: <https://earthexplorer.usgs.gov/> (Accessed 14 August 2017), 2017.
- 551 USGS: NHDPlus High Resolution, [online] Available from: [https://nhd.usgs.gov/NHDPlus\\_HR.html](https://nhd.usgs.gov/NHDPlus_HR.html) (Accessed 29 June 2018),  
552 2012.
- 553 Van Meter, K. J. and Basu, N. B.: Catchment Legacies and Time Lags: A Parsimonious Watershed Model to Predict the Effects  
554 of Legacy Storage on Nitrogen Export, edited by Y. Hong, *PLoS ONE*, 10(5), e0125971, doi:10.1371/journal.pone.0125971, 2015.
- 555 Van Meter, K. J. and Basu, N. B.: Time lags in watershed-scale nutrient transport: an exploration of dominant controls,  
556 *Environmental Research Letters*, 12(8), 084017, doi:10.1088/1748-9326/aa7bf4, 2017.
- 557 Verstraeten, I. M., Sibray, S. S., Cannia, J. C. and Tanner, D. Q.: Reconnaissance of ground-water quality in the North Platte  
558 Natural Resources District, western Nebraska, June-July 1991, Report, United States Geological Survey. [online] Available from:  
559 <http://pubs.er.usgs.gov/publication/wri944057>, 1995.
- 560 Verstraeten, I. M., Steele, G. V., Cannia, J. C., Hitch, D. E., Spreter, K. G., Böhlke, J. K., Kraemer, T. F. and Stanton, J. S.:  
561 Interaction of surface water and ground water in the Dutch Flats area, western Nebraska, 1995-99, Report, United States Geological  
562 Survey. [online] Available from: <http://pubs.er.usgs.gov/publication/wri014070>, 2001a.
- 563 Verstraeten, I. M., Steele, G. V., Cannia, J. C., Böhlke, J. K., Kraemer, T. E., Hitch, D. E., Wilson, K. E. and Carnes, A. E.: Selected  
564 field and analytical methods and analytical results in the Dutch Flats area, western Nebraska, 1995-99, Report, United States  
565 Geological Survey, Reston, VA. [online] Available from: <http://pubs.er.usgs.gov/publication/ofr00413>, 2001b.
- 566 Welch, H. L., Green, C. T. and Coupe, R. H.: The fate and transport of nitrate in shallow groundwater in northwestern Mississippi,  
567 USA, *Hydrogeology Journal*, 19(6), 1239–1252, doi:10.1007/s10040-011-0748-8, 2011.
- 568 Wells, M., Gilmore, T., Mittelstet, A., Snow, D. and Sibray, S.: Assessing Decadal Trends of a Nitrate-Contaminated Shallow  
569 Aquifer in Western Nebraska Using Groundwater Isotopes, Age-Dating, and Monitoring, *Water*, 10(8), 1047,  
570 doi:10.3390/w10081047, 2018.
- 571 Wheeler, D. C., Nolan, B. T., Flory, A. R., DellaValle, C. T. and Ward, M. H.: Modeling groundwater nitrate concentrations in  
572 private wells in Iowa, *Science of The Total Environment*, 536, 481–488, doi:10.1016/j.scitotenv.2015.07.080, 2015.
- 573 Yonts, D.: G02-1465 Crop Water Use in Western Nebraska, University of Nebraska-Lincoln Extension [online] Available from:  
574 <https://digitalcommons.unl.edu/extensionhist>, 2002.
- 575 Young, L.A. (UNL): Personal Communication with M.J. Wells, University of Nebraska, Lincoln, NE, USA, 2016.
- 576
- 577
- 578



579  
580 **Figure 1: Dutch Flats study area overlain by 30 m Digital Elevation Model (NeDNR 1997). Depending on data availability, multiple wells**  
581 **(well nest) or a single well may be found at each monitoring well location.**



582



583

584

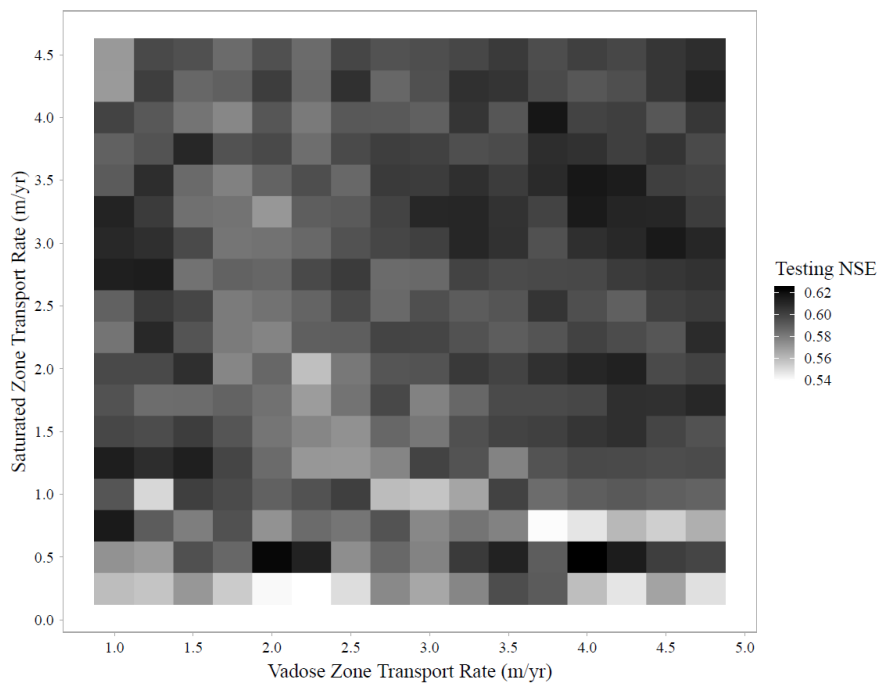
585

**Figure 2: Time series plots of all four dynamic predictors. Starting in the upper left and moving clockwise, figures represent annual precipitation, canal discharge, center pivot irrigation and area of plant corn from 1946 to 2013.**

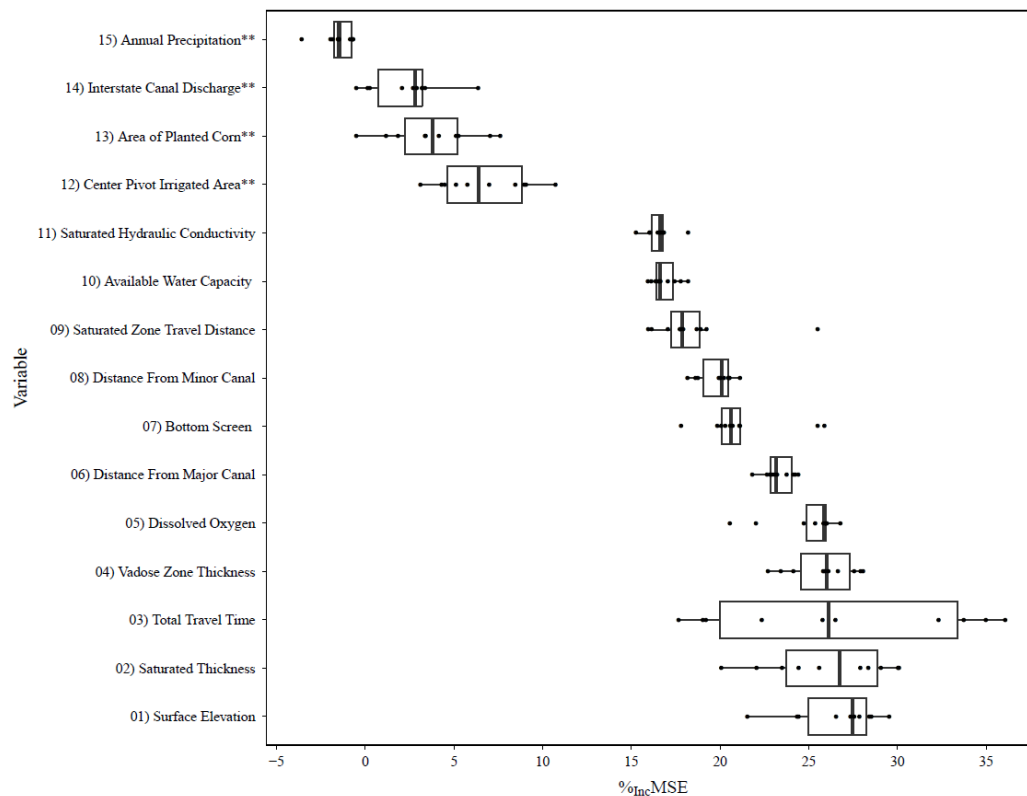
586



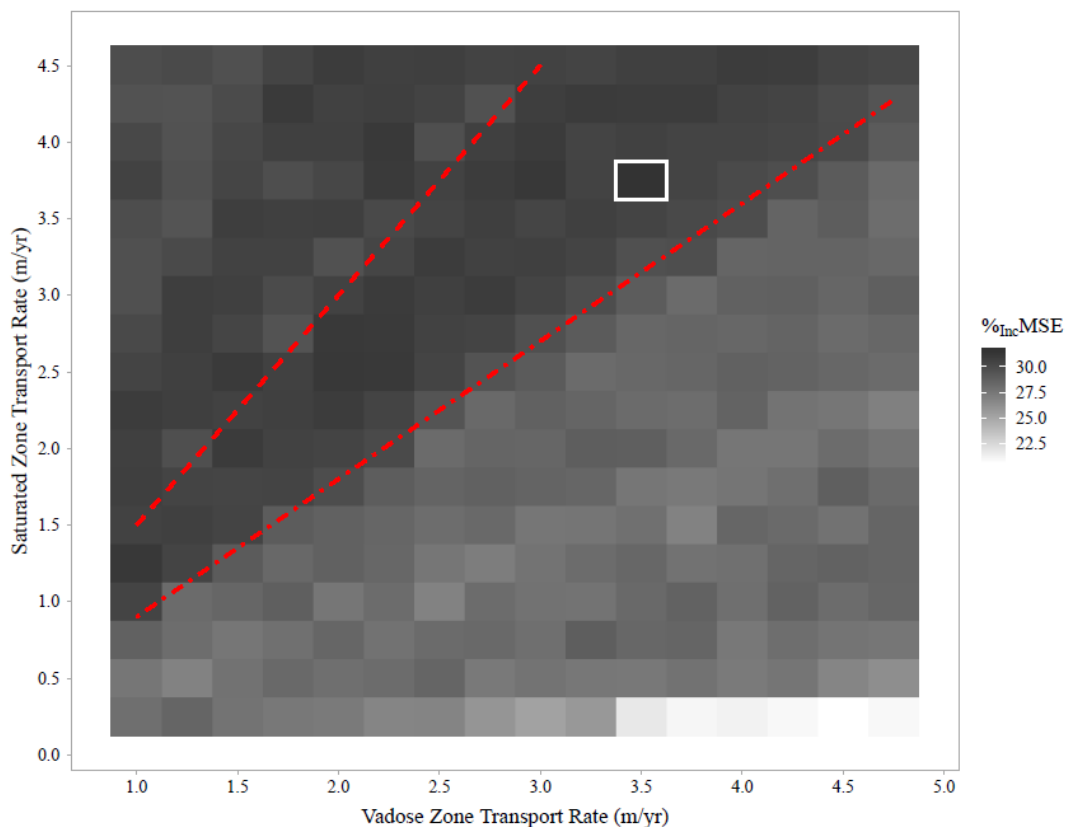
587



588  
589 **Figure 3: Heat map of testing NSE results from 288 vadose and saturated-zone transport rate combinations. Testing NSE in this figure**  
590 **is the median of all 25 model outputs from each of the 288 transport rate combinations. No clear pattern of optimal vadose and saturated-**  
591 **zone transport rate combinations was observed.**

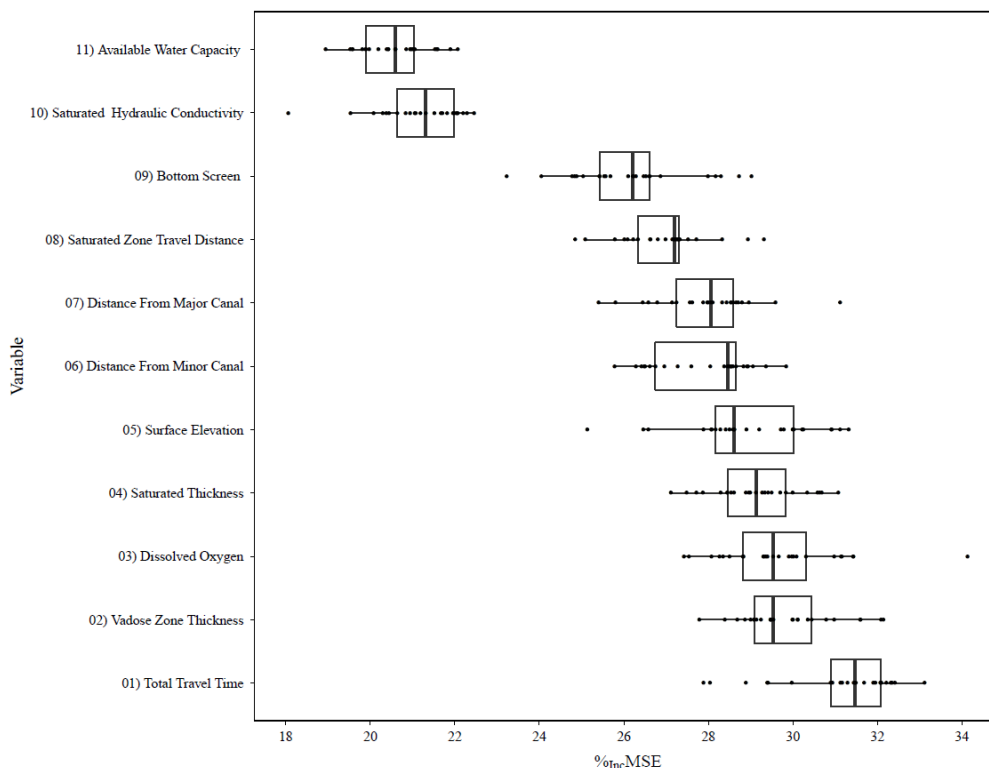


592  
593 **Figure 4: Boxplot of the %IncMSE from the ten transport rate combinations shown in Table 2. Each boxplot has ten points for each**  
594 **transport rate combination, representing the median %IncMSE from the 25 models (five-fold cross validation, repeated 5 times). A larger**  
595 **%IncMSE suggests the variable had a greater influence on a model's ability to predict [NO<sub>s</sub>]. \*\*Denotes dynamic predictors.**



596  
597 **Figure 5: Heat map of %<sub>inc</sub>MSE (median from 25 models) from variable importance of total travel time for each of the 288 transport**  
598 **rate combinations evaluated. Red dashed lines indicate upper ( $V_s / V_u = 1.5$ , long dashes) and lower (0.9, short dashes) bounds of the**  
599 **band of transport rate combinations with consistently higher %<sub>inc</sub>MSE. The white square highlights the single transport rate**  
600 **combination with the highest %<sub>inc</sub>MSE.**

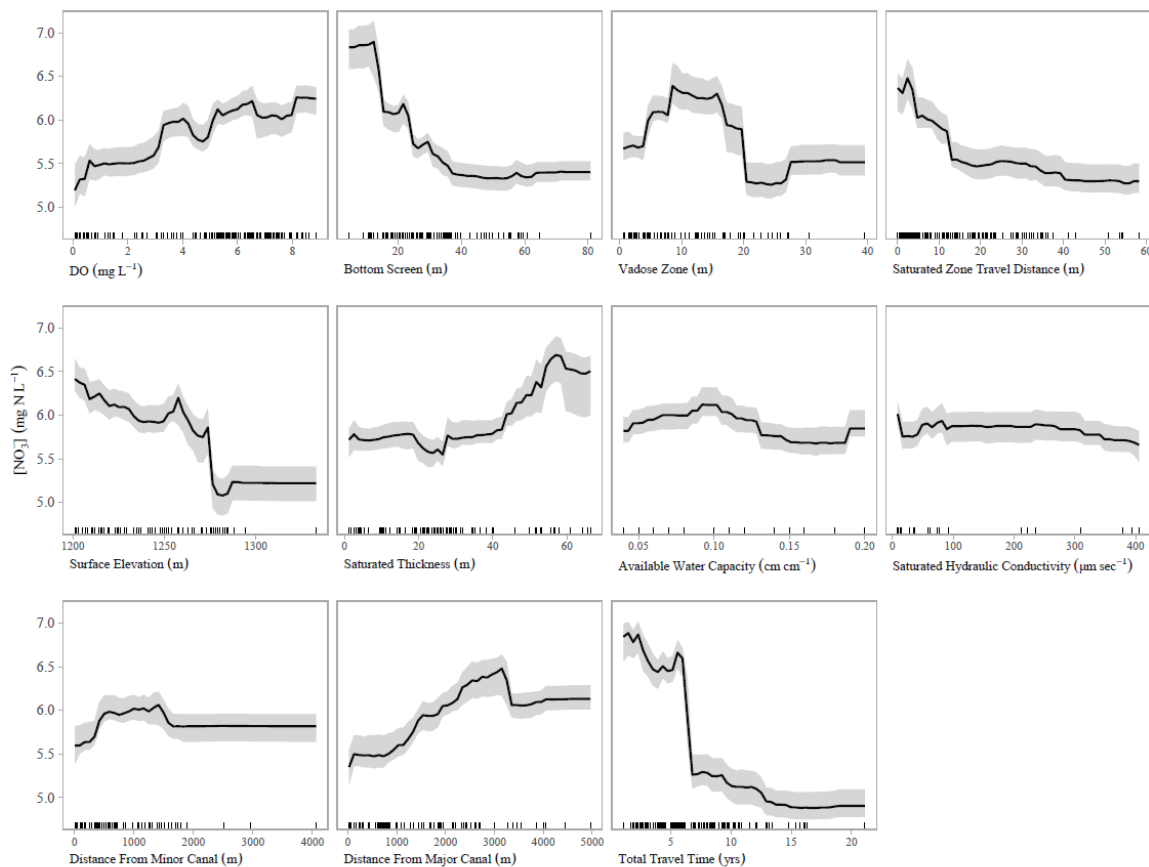
601



602  
603 **Figure 6: Plot from secondary analysis exploring variable importance of the transport rate combination with the largest median**  
604 **%<sub>IncMSE</sub> in total travel time ( $V_u = 3.5$  m/yr;  $V_s = 3.75$  m/yr). Each point is from one of 25 Random Forest models run for this evaluation.**  
605 **A larger %<sub>IncMSE</sub> suggests the variable had a greater influence on a model's ability to predict  $[NO_s^-]$ .**

606

607



608  
609 **Figure 7: Partial dependence plot for model evaluating transport rate combination of  $V_u = 3.5$  m/yr and  $V_s = 3.75$  m/yr. Tick marks on**  
610 **each plot represent predictor observations used to train models.**

611  
612  
613  
614  
615  
616  
617  
618  
619  
620



621 **Table 1. List of the 15 predictors used for Random Forest evaluation. Average (avg.) and median (med.) values are shown.**  
 622

Predictor	Units	Predictor Type	Source
Center Pivot Irrigated Area (avg. = 2618; med. = 1037) <sup>a</sup>	hectare	Dynamic	NAIP; NAPP; Landsat-1,5, 7, 8 <sup>b</sup>
Interstate Canal Discharge (avg. = 0.53; med. = 0.55) <sup>a</sup>	km <sup>3</sup> yr <sup>-1</sup>	Dynamic	USBR (2018)
Area of Planted Corn (avg. = 8065; med. = 7869) <sup>a</sup>	hectare	Dynamic	NASS (2018)
Precipitation (avg. = 384; med. = 377) <sup>a</sup>	mm yr <sup>-1</sup>	Dynamic	NOAA (2017)
Available Water Capacity (avg. = 0.1; med. = 0.1)	cm cm <sup>-1</sup>	Static	NRCS (2018)
Dissolved Oxygen (avg. = 4.6; med. = 5.4)	mg L <sup>-1</sup>	Static	C. Hudson, Personal Communication (2018)
Distance from a Major Canal (avg. = 1462.2; med. = 1161.4)	m	Static	USGS (2012) <sup>b</sup>
Distance from a Minor Canal (avg. = 633.2; med. = 397.6)	m	Static	USGS (2012) <sup>b</sup>
Bottom Screen (avg. = 26.9; med. = 24.4)	m	Static	NEDNR (2016) <sup>b</sup>
Saturated Hydraulic Conductivity (avg. = 68; med. = 28)	µm sec <sup>-1</sup>	Static	NRCS (2018)
Saturated Thickness (avg. = 30.2; med. = 27.6)	m	Static	T. Preston, Personal Communication (2017) <sup>b</sup>
Saturated-Zone Travel Distance (avg. = 13.3; med. = 7)	m	Static	NEDNR (2016) <sup>b</sup>
Surface Elevation (DEM) (avg. = 1244; med. = 1248)	m	Static	NEDNR (1997)
Total Travel Time (avg. = 6.4; med. = 5.7) <sup>c</sup>	years	Static	NEDNR (2016) <sup>b</sup>
Vadose-Zone Thickness (avg. = 9.9; med. = 7.3)	m	Static	T. Preston, Personal Communication (2017); A. Young, Personal Communication (2016)

<sup>a</sup> Average and median span from 1946 to 2013

<sup>b</sup> Data required further analysis to yield calculated values; data sources are USDA (2017) and USGS (2017)

<sup>c</sup> Average and Median reflects transport rates of  $V_u = 3.5$  m/yr and  $V_u = 3.75$  m/yr

623

624 **Table 2. Summary of ten vadose and saturated-zone transport rate combinations selected from 288 unique potential combinations.**

	Vadose-zone Transport Rate (m/yr)	Sat. Zone Transport Rate (m/yr)	Test NSE	[NO <sub>3</sub> ] <sup>-</sup> Observations <sup>a</sup>	Total Travel Time (yrs)	
					Mean (±1σ)	Median
Five Top-Performing Transport Rates	4.00	0.50	0.623	878	19.9 (± 15.8)	11.3
	2.00	0.50	0.622	861	21.6 (± 15.0)	16.5
	3.75	4.00	0.617	1049	6 (± 3.7)	5.4
	4.00	3.50	0.617	1049	6.3 (± 4.1)	5.7
	4.50	3.00	0.616	1049	6.7 (± 4.7)	5.7
Extreme and Midrange Transport Combinations	4.75	4.50	0.608	1049	5.1 (± 3.2)	4.6
	2.75	2.25	0.599	1049	9.6 (± 6.3)	8.5
	1.00	4.50	0.570	1049	12.6 (± 7.7)	10.8
	1.00	0.25	0.559	607	26.7 (± 13.3)	20.6
	4.75	0.25	0.548	664	21.3 (± 15.0)	14.9

625 <sup>a</sup>In cases with low transport rates, lag times were relatively long and not all historical data could be used in the model. Thus, some models were ultimately based  
 626 on <1,049 observations.  
 627